# Accepted (peer-reviewed) Version

# Perovskite Solar Cells: Stable under Space Conditions

Daniel Pérez-del-Rey[1], Chris Dreessen[1], Ana M. Igual-Muñoz[1], Lennart van den Hengel[2], María C. Gélvez-Rueda[2], Tom J. Savenije[2], Ferdinand C. Grozema[2], Claus Zimmermann[3] and Henk J. Bolink[1,*]

1: Instituto de Ciencia Molecular, Universidad de Valencia, C/ Catedrático J. Beltrán 2, 46980 Paterna, Spain.

2: Department of Chemical Engineering, Delft University of Technology, Van der Maasweg 9, 2629 HZ, Delft, The Netherlands.

3: Airbus DS, 81663 Munich, Germany.

Abstract:

Metal halide perovskite solar cells are of interest for high altitude and space applications due to their light weight and versatile form factor. However, their resilience towards the particle spectrum encountered in space is still of concern. For space cells, the effect of these particles is condensed into an equivalent 1 MeV electron fluence. We probe the effect of high doses of 1 MeV e-beam radiation up to an accumulated fluence to $10^{16}$ e/cm$^2$ on methylammonium lead iodide perovskite thin films and solar cells. By using substrate and encapsulation materials that are stable under the high energy e-beam radiation we can study its net effect on the perovskite film and solar cells. Our quartz substrate-based perovskite solar cells are stable under the high doses of 1 MeV e-beam irradiation. Time resolved microwave conductivity analysis on pristine and irradiated films indicate that there is a small reduction in the charge carrier diffusion length upon irradiation. Nevertheless this diffusion length remains, larger than the perovskite film thickness used in the solar cells, even for the highest accumulated fluence of $10^{16}$ e/cm$^2$. This demonstrates that perovskite solar cells are promising candidates for space applications.

Thin film metal halide perovskite solar cells (PSCs) have reached power conversion efficiencies as high as 25 % for single junction solar cells.[1,2,3] Similar efficiencies have been reached for multi-junction cells using two different perovskite absorbers.[4,5] For these multi-junction cells, it is expected that much higher efficiencies can be reached by reducing losses from the wide bandgap subcell.[6,7,8] Due to the high absorption coefficient and direct bandgap the perovskite films are rather thin, in the range of 0.5 micrometers.[9] This implies that the complete solar cell stack is generally less than 1 micrometer thick if we exclude the substrate. Hence, when employed on a thin and light weight substrate their power to weight ratio can be very high (26 W/g) for a 4 μm thick polyester substrate.[10] These properties make perovskite solar cell very appealing for high altitude and space applications. In space applications the solar cells are exposed to high energy radiation and it is therefore crucial to evaluate their stability under such conditions. In one case PSCs were tested in the stratosphere by elevating them using a balloon flight. The power conversion efficiency (PCE) dropped with 36 % after the balloon flight.[11] Several accelerated tests exposing the solar cells to high doses of high energy radiation using electrons,[12] protons,[13,14] neutrons,[15] and gamma-rays[16] have also been performed in PCSs. In all but one case, the initial PCE of the employed cells was in between 5 and 14 %, which may not be representative as only high-efficiency PSCs will eventually be used in space missions. Even though the results on these cells are in general positive, there are still considerable uncertainties. Additionally, a number of studies using lower energy (keV) electron beams, in general those used in scanning electron microscopy, have shown structural changes in solution processed perovskite films.[12,17,18] The damage in these experiments is caused by the high accumulated dose rates, in the order of $1x10^{18}$ to $1x10^{20}$ $e^{-} cm^{-2}$. In addition, the energy deposition for keV electron beams is very different from 1MeV electrons. At these low energies the penetration depth is much less, which is likely to lead to more direct damage in the perovskite layer. According to the standard space solar cell qualification and quality

requirements, AIAA S-111A-2014/A1-2019, the tests to predict degradation in space require the use of high energy electron irradiation. These conditions were used recently to evaluate solution processed PSC with a high PCE.[19] In that study the initial PCE was around 20 % and thus significantly above that of previously studied PSCs which were studied under various irradiation conditions. Upon exposure to 1 MeV e-beam with an accumulated fluence up to $10^{15}$ e/cm$^2$, a significant reduction in the PCE of the solar cells was observed. This was caused by a modest reduction in the open circuit voltage ($V_{oc}$) and fill factor (FF) but primarily by a strong reduction in the short circuit current ($J_{sc}$). The strong decrease of the $J_{sc}$ upon irradiation was a combination of irradiation induced darkening of the soda lime glass used as the substrate and perovskite degradation.

In this work we demonstrate beyond any doubt that PSCs are stable under high doses of 1 MeV e-beam radiation conditions. We do this by investigating high efficiency vacuum deposited methyl ammonium lead iodide ($MAPbI_3$) based PSCs on both soda lime and quartz substrates and by extending the accumulated fluence to $10^{16}$ e/cm$^2$. Under these conditions, the quartz substrate-based PSC show virtually no degradation. Surprisingly, we find in our study of more than 60 cells; that those show initially slightly lower performance improve after e-beam exposure, whereas top performing cells remain unchanged.

**Results**

The $MAPbI_3$ films were characterized using x-ray diffraction (XRD), scanning electron microscopy (SEM) upon preparation. In figure 1 the typical x-ray diffractogram is depicted for the pristine film. The reference sample has the typical diffraction patterns for this perovskite, highly oriented along the 001 direction (Figure 1a). The $MAPbI_3$ also exhibited the typical grain structures (Figure 1b) and spectroscopic features (Figure S1).[20]

The typical performance of the solar cells employing the films is similar as previously reported[21] and the current density (J) versus voltage (V) curves when illuminated with 1 sun of AM1.5 spectrum are displayed in Figure 1d. The key performance parameters derived from the J-V curve are as follows: $J_{sc}$ of 20.6 mA/cm$^2$, $V_{oc}$ of 1.16 V and FF of 78% leading to a PCE of 18.6 %.

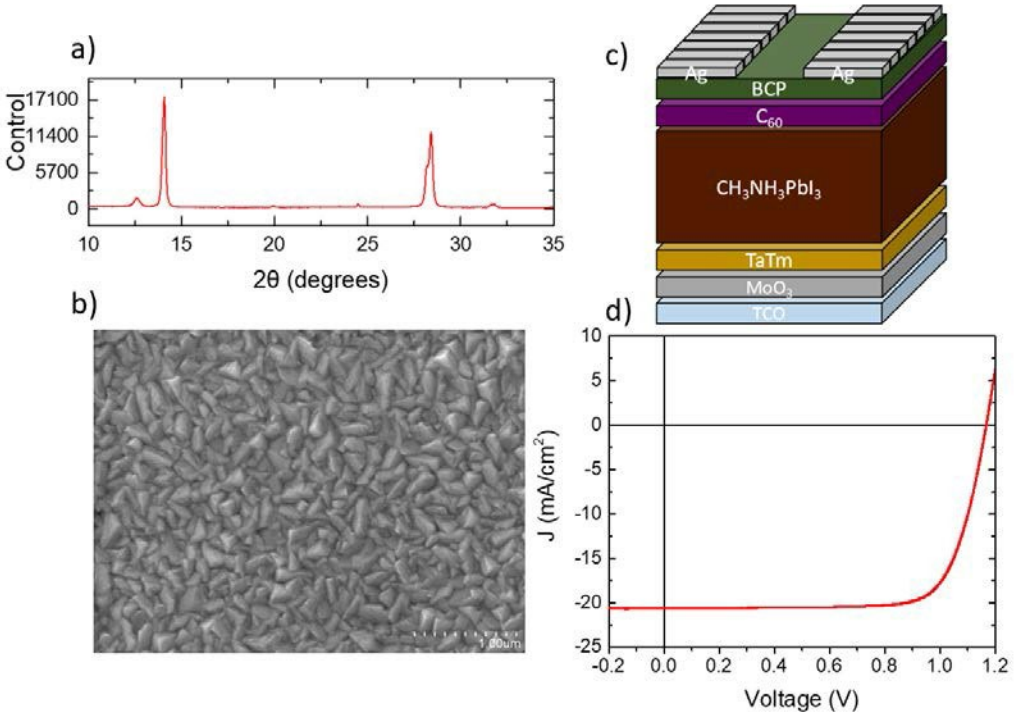


Figure 1: a) XRD diffraction pattern of the sublimed $MAPbI_3$ film capped with 50 nm of PMMA, b) Scanning electron microscope image of perovskite deposited on glass. c) Schematic of the used solar cell layout: ITO / $MoO_3$ (5 nm) / TaTm (10 nm) / $CH_3NH_3PbI_3$ (600 nm) / C60 (25 nm) / BCP (7 nm) / Ag d) J-V curve under AM1.5 illumination at 1 sun intensity.

The first irradiation experiments were done using solar cells that were deposited on ITO coated glass substrates. These were irradiated (radiation incident on the glass ITO side of the device) with 1 MeV electrons reaching fluences of $10^{14}$ and $10^{15}$ e/cm$^2$. To ensure that the encapsulation is robust enough and sample shipment from Valencia to Delft and back is not affecting the performance, control devices were also included in the experiments. The irradiation

experiments were performed using 1 MeV electrons from a Van de Graaf electron accelerator, at 20 °C, for approximately 200 and 2000 seconds ($5 \cdot 10^{11}$ $e^{-}s^{-1}cm^{-2}$), for the $10^{14}$ and $10^{15}$ $e^{-}/cm^{2}$, respectively. The use of soda lime glass as the substrate introduces a complication since it contains impurities. These impurities act as traps for electrons and holes in the materials generated by the high energy electron irradiation, leading to color centers in the material.[22] These are long-lived trapped charges that absorb in the visible and hence leads of a progressive darkening of the substrate with higher accumulated fluences (Figure 2a). This led to a reduction in the $J_{sc}$ going from 20 to 14 and 12 $mA/cm^{2}$, respectively for the two fluences employed. Interestingly, the FF is virtually unaffected by the irradiation or, if anything, it leads to an increase in FF(Figure 2c).

The $V_{oc}$ is slightly reduced, from 1.14 to 1.11 V upon irradiation (Figure 2b and 2c). This minor decrease can be accounted for by the reduction of the $J_{sc}$. As a result of the strong reduction in $J_{sc}$ the PCE of the solar cells drops from an average value of 18 % to 12 and 10 % for the cells exposed to e-beam radiation of fluences reaching $10^{14}$ and $10^{15}$ $e/cm^{2}$, respectively. The variation in the performance parameters for the different cells is very small as can be observed from Figure 2c with most of the cells that were evaluated showing a similar performance as a function of irradiation dose.

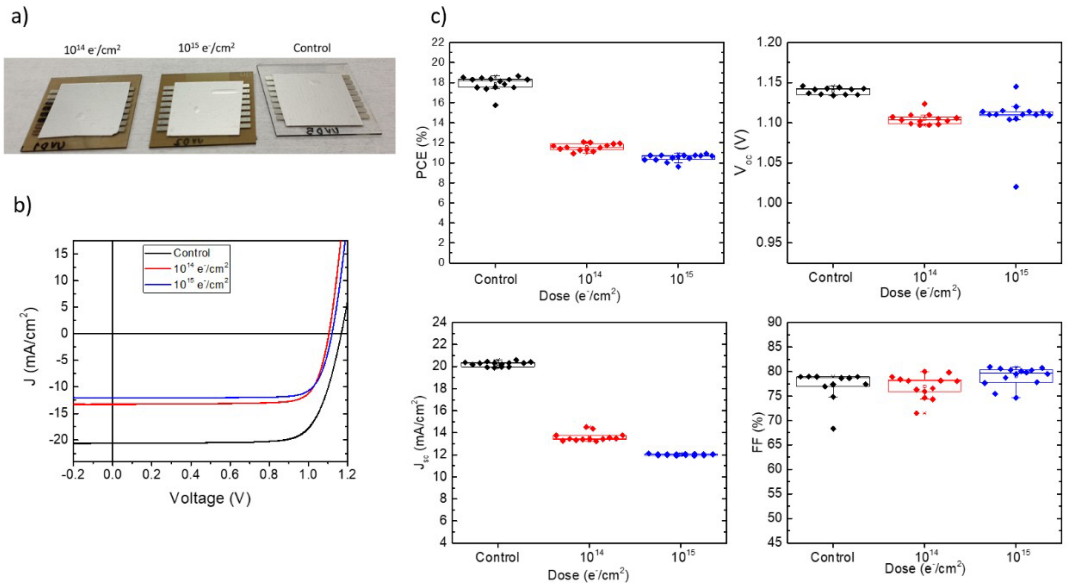


Figure 2: Performances for devices on soda lime glass a) images of the reference and e-beam exposed solar cells, b) J-V curves under AM1.5 illumination at 1 sun intensity, c) PCE, $J_{sc}$, $V_{oc}$ and FF derived from the J-V curves and plotted as a function of electron beam fluence. The control devices were also shipped and kept in air for the same duration as the longest e-beam irradiation experiment.

For confirmation of the suspected darkening of the glass substrates as cause of the reduction in $J_{sc}$ and, more importantly, for the study of PSC without this artefact, a second series of devices were prepared on ITO coated quartz substrates. The initial performance is similar, yet the best performing cells had a PCE of 19 %, hence slightly higher than those prepared on glass substrates. This slight increase is not the effect of the substrate but rather some small fluctuation in device performance over time. We attribute these slight changes to the use of different batches of $PbI_2$ and MAI as the second series of e-beam experiments was performed several months after the first set of experiments. For this second batch of cells we extended the accumulated electron fluence up to $10^{16}$ $e^-/cm^2$. The radiation was again incident on the ITO side (now on the quartz substrates) of the devices. As the control devices on glass substrates did not show degradation during shipping and exposure to air, they were omitted in this second batch of PSCs on quartz substrates. Compared to the previous batch, the variation in performance of

the as-prepared cells is slightly increased. The PCE varies from 16 to 19 %. The origin of the increased variation is not fully understood but is in part due to the patterning of the ITO which was done manually instead of using industrial photolithography as in the case of the ITO on glass substrates.

Several substrates and a multitude of cells were irradiated with 1 MeV electrons reaching fluences of $10^{14}$, $10^{15}$ and $10^{16}$ $e^-/cm^2$. The J-V curves (under 1 sun illumination) of a control cell and irradiated cells are depicted in Figure 3a. Both forward and reverse scans are virtually the same for all accumulated fluences, the key performance parameters for these curves differ only marginally leading to a PCE of 18-18.5 %. See Table S1 for the averages of the performance indicators for each accumulated fluence. Hence, the performance of the devices remains virtually identical even when irradiated with the highest accumulated fluence of $10^{16}$ $e^-/cm^2$. For The actual particle spectrum in space consists of protons and electrons with a broad range of energies. For III-V space cells, the effect of these particles is condensed into one equivalent 1 MeV electron fluence, based on the non-ionizing energy loss deposited in the material. For typical space missions this results in equivalent fluences around $10^{15}$ $e^-/cm^2$, with fluences around $10^{14}$ $e^-/cm^2$ encountered in low earth orbit missions, and $10^{16}$ $e^-/cm^2$ for missions in the inner radiation belts. For PSC these relative damage coefficients, correlating the effect of different energies of one particle type as well as the relative effect between electron and protons still needs to be determined. Nevertheless, the fact that no degradation is observed for a dose of $10^{16}$ $e^-/cm^2$ implies that perovskite solar cells are promising candidates for space applications. These findings compare favourably with results obtained under similar conditions for Si,[23] GaAs,[24] and InGaP/InGaAs/Ge,[25] single and triple junction cells that show a larger decrease of the overall efficiency (10-30%). Other thin film technologies like CdTe and Cu(In,Ga)Se (CIGS) show similar stability than our perovskite solar cells. CdTe showed 4% degradation in overall efficiency at $2x10^{16}$ $e^-$ $cm^{-2}$.[26] And CIGS cells on glass have been found to be stable up to $1x10^{17}$ $e^-$ $cm^{-2}$ 1 MeV electron irradiation.[27]

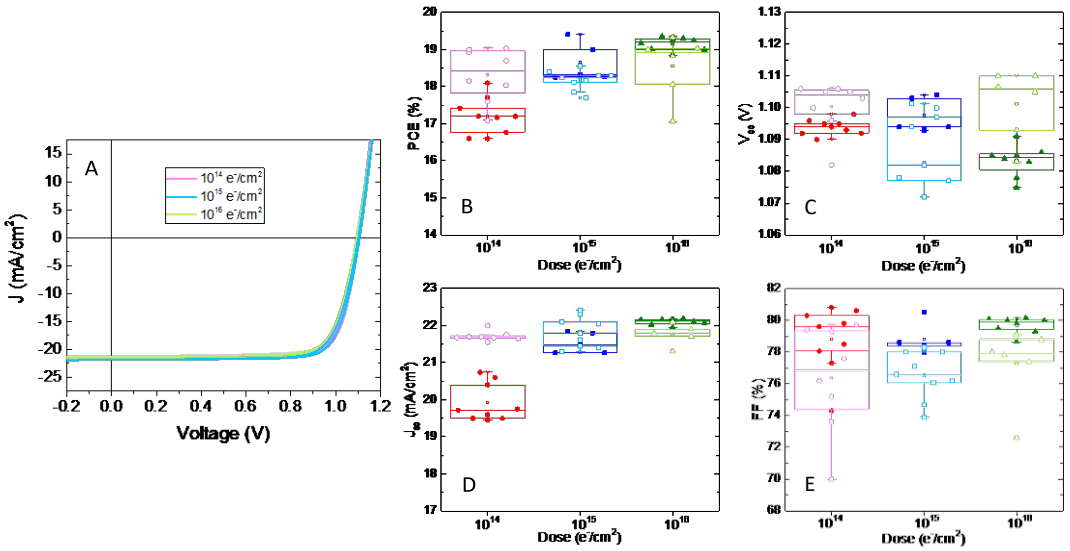


Figure 3: Quartz substrate based PSCs. A) J-V curves obtained under 1 sun illumination for solar cells exposed to different accumulated high energy eV fluences. B, C, D and E) PCE, Jsc, Voc and FF versus accumulated electron fluence, respectively of the quartz substrate based solar cells. Closed symbols are the values before irradiation and open symbols are after irradiation.

All the irradiation doses shown were tested on 2 equal devices with more than 10 pixels each to discard any effect of the encapsulation and have reliable data (see Table S1 for average data). As mentioned, for the quartz-based PSCs the variation in performance was larger than for the first batch on glass substrates, there were also a number of pixels with large leakage currents that were discarded from the analysis. Another result of this variation is that not all cells had the same PCE prior to the irradiation experiments. This variation, although undesired, has allowed us to observe an unexpected behaviour of the PSCs. Namely, the PSC with a lower initial performance become better after irradiated with MeV electrons. This effect can be clearly observed for the cells irradiated with an accumulated dose of $10^{14}$ e/cm$^2$. For these cells, both the $J_{sc}$ and $V_{oc}$ increase, whereas the FF slightly decreases.

A decrease of the FF is generally observed for all cells exposed to different irradiation doses. The $J_{sc}$ when initially in between 21 and 22 mA/cm$^2$ is not significantly affected by the irradiation, independent on the accumulated fluence reached. Only when the $J_{sc}$ is low on the pristine cells, it increases upon irradiation. There is also a notable increase in the $V_{oc}$ for the cells exposed to accumulated fluences of $10^{14}$ and $10^{16}$ $e^-/cm^2$. Unfortunately, the variation of data for the cells exposed to accumulated fluences of $10^{15}$ $e^-/cm^2$ is too large to draw conclusions from it. However, for the other two accumulated fluences, below and above $10^{15}$ $e/cm^2$ the effect is clear, which we therefore assume to be a general trend for all accumulated fluences. Due to this "healing" effect on $J_{sc}$, which compensates for the loss in FF, the overall PCE of the solar cells remains unchanged upon irradiation.

The penetration depth of the high energy electrons is much larger than the thickness of the used quartz plates (0.7 mm) and therefore eventually all electrons reach the perovskite layer. The effect of radiation can actually only be related to the cell as a whole. The perovskite layer is so thin (0.6 μm) that almost no direct ionizations will take place for 1MeV electrons. However, there are indirect effects; the passing of the electrons through quartz will generate Cerenkov radiation (wide range of wavelengths peaking in the UV) which will be absorbed in the perovskite and can lead to damage. In addition, backscattering from the aluminum back electrode will result in some low-energy electrons that will deposit energy (ionizations) in the perovskite. Therefore, on the cell-level we can only see the overall effect of the irradiation dose and can not link it to one particular section or layer within the device stack. We performed some additional experiments on irradiated devices and on the perovskite films to try and elucidate if some evidence for high energy radiation related structural degradation in the perovskite layer can be found. Analysis of the irradiated $MAPbI_3$ films using XRD and SEM did not reveal any significant change in the crystallinity or grain morphology (Figure S2 and S3). The steady state photoluminescence spectra of the irradiated devices were measured using an excitation wavelength of 350 nm with a bandwidth of 7 nm and a wide emission range from 380 to 910

nm. The photoluminescence signal of the HTL used, TaTm, appears around 450 nm and is identical in shape for all irradiation doses (Figure S1 for a typical curve). The typical photoluminescence of $MAPbI_3$ is observed at 769 nm and also does not change significantly with irradiation dose. Hence, no detectable damage can be observed from the PL spectra. A sensitive external quantum efficiency (EQE) measurement in the bandgap region for solar cells exposed to different irradiation fluences did not show any additional trap states (Figure S5). Hence, even though these are sensitive techniques we were unable to determine significant changes upon irradiation. By taking the first derivative of the EQE spectrum an accurate determination of the perovskite bandgap is obtained which is 1.60 eV in agreement with previous reports (Figure S6).

In an attempt to gain more insight in the effect of exposure to 1 MeV electron on the electronic properties of the intrinsic perovskite layer we have performed time-resolved microwave conductivity measurements (TRMC). The perovskite samples were deposited on quartz substrates by vacuum deposition in the same way as for the solar cells discussed above, and subsequently sealed with a poly(methyl methacrylate) (PMMA) layer by spin-coating. This sealing is done to prevent degradation due to exposure to oxygen and water under ambient conditions. Figure 4 shows a comparison of the photoinduced conductivity in perovskite samples using the TRMC technique for different doses of irradiation with 1 MeV electrons. The samples were excited with a 3.5 ns laser pulse ($\lambda$ = 650 nm) resulting in an increase in conductivity upon photogeneration of charges. After the excitation pulse, the conductivity decays due to a recombination and trapping of charges. The differences in the decay of the photo-conductivities for different irradiation doses is relatively small, however, there is a clear trend, showing slightly faster decay for the highest doses. Exponential fits of decays show a small but gradual decrease of the decay time from ~55 ns for the unirradiated samples to ~40 ns for the sample irradiated with $10^{16}$ $e^-/cm^2$. This points to the formation of trapping sites in the perovskite material itself. This trap formation is supported by additional TRMC measurements for varying laser excitation densities (see Figure S7). These show that for the non-irradiated sample, there is a clear higher

order recombination effect, leading to faster decay for higher initial charge densities. For the sample irradiated with $10^{16}$ $e^-/cm^2$ this second order effect is significantly less pronounced, indicating more first order decay by trapping. From the carrier mobility and lifetime obtained from the TRMC measurements, the carrier diffusion length can be derived, as shown in Table S2. The estimated carrier diffusion lengths range from ~0.8 μm for the non-irradiated sample, down to ~0.65 μm for the $10^{16}$ $e^-/cm^2$ sample. The latter diffusion length is still well-above the thickness of the perovskite layer in the solar cells studied here, consistent with the small effect of irradiation on the solar cells efficiency.

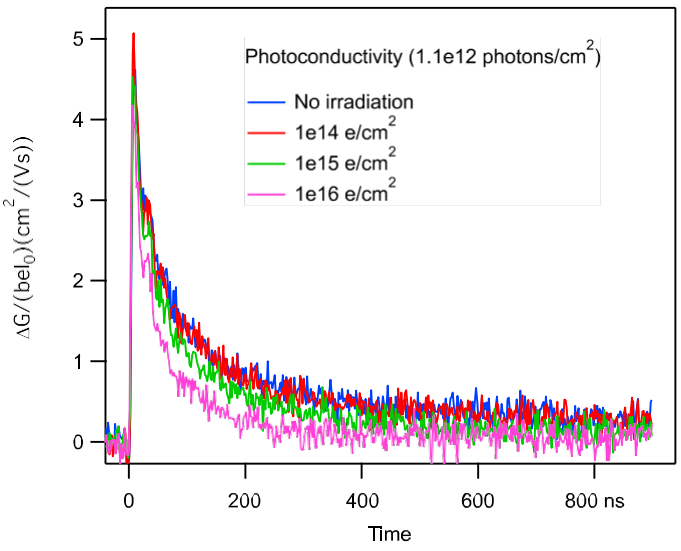


Figure 4: Photoinduced conductivity of perovskite samples on quartz capped with PMMA from time-resolved microwave photoconductivity measurements for the control film and those exposed with the indicated electron irradiation doses.

In conclusion, we have prepared two sets of thin film perovskite based solar cells employing vacuum sublimation for all the materials. The first set employed glass based substrates whereas the second set was prepared using quartz substrates. The glass based perovskite solar cells darkened significantly during irradiation experiments. This leads to a decrease in solar cells performance but it is not clear if this originates solely from the darkened substrate or also from

degradation of the solar cells themselves. The quartz substrate based cells do not darken upon irradiation and allow for a careful analysis of the effect of the irradiation fluences on the solar cell performance. The main finding is that these fully vacuum deposited perovskite solar cells maintain their high power conversion efficiency of 19 % after irradiation with high energy electrons up to very high accumulated fluence ($10^{16}$ e/cm$^2$). This implies that perovskite solar cells are promising candidates for space applications. Detailed studies do show that there is a slight reduction in the fill factor which is compensated by an increase in the open circuit voltage. Surprisingly, we find that cells that exhibit performances at the bottom of the distribution are improved after having been irradiated. This improvement is primarily due to an increase in open circuit voltage. Time resolved microwave conductivity analysis on pristine and irradiated films indicate that there is a small reduction in the charge carrier diffusion length upon irradiation. Nevertheless this diffusion length remains, larger than the perovskite film thickness used in the solar cells, even for the highest accumulated fluence of $10^{16}$ e/cm$^2$. This explains why no reduction in solar cells performance is observed under these conditions.

## Methods

Photolithographically patterned ITO coated glass substrates were purchased from Naranjo Substrates. N4,N4,N4',N4'-tetra([1,1'-biphenyl]-4-yl)-[1,1':4',1'-terphenyl]-4,4'-diamine (TaTm) was provided by Novaled GmbH. Fullerene ($C_{60}$) was purchased from sigma Aldrich. $PbI_2$ was purchased from Tokyo Chemical Industry CO (TCI), while $CH_3NH_3I$ (MAI), $MoO_3$ and bathocuproine (BCP) were purchased from Lumtec. ITO on quartz substrate were purchased from Präzisions Glas & Optik GmbH and patterned in-house using a soft etching process.

Thin (600 nm) $MAPbI_3$ films were formed by dual-source vacuum deposition of MAI and $PbI_2$ following the procedure used to obtain high efficiency solar cells reported previously.[28] These $MAPbI_3$ films were integrated in p-i-n type planar solar cells, by depositing them onto an ITO coated substrates of 3 by 3 cm covered with 5 nm of $MoO_3$ and 10 nm of TaTm. Following the perovskite deposition, the devices were completed by depositing 25 nm of $C_{60}$, 7 nm of BCP and

100 nm of Ag (Figure 1c). All layers were deposited using thermal sublimation in an inert atmosphere integrated vacuum chamber (see experimental section for more details). After preparation the cells were encapsulated using a thin (0.8 mm) aluminium sheet and an adhesive (Figure 2a). To allow evaluating just the 600 nm $MAPbI_3$ films without degrading them during the irradiation test, they were covered with a thin (50 nm) polymethylmethacrylate (PMMA) film. The PMMA was deposited by spincoating at 3000 rpm from a toluene solution of ~40 mg/ml. Prior to the SEM analysis of the irradiated films, the PMMA film was removed by washing with toluene.

The solar cells were characterized through a shadow mask with 0.05 $cm^2$ aperture using a WaveLabs Sinus 50 solar simulator with spectral response matching AM1.5G illumination (see for details the experimental section). High energy electron beam radiation (1 MeV) experiments were performed Van de Graaf electron accelerator facility at Delft University of Technology. Hence, after preparation of the cells, they were transported from Valencia to Delft in a nitrogen filled sealed transport container. The solar cells are irradiated from the top quartz side to the bottom aluminum side of the device stack. The cells are placed on an irradiation table covered with a frame with kapton foil window (50 μm) for irradiation under inert gas conditions (nitrogen flow at 10 l /min). The irradiation dose and time of exposure depends on the accumulated dose desired. For the accumulated doses of $1x10^{14}$ $e^-$ $cm^{-2}$ and $1x10^{15}$ $e^-$ $cm^{-2}$ the solar cells and perovskite films were exposed to an irradiation dose of 5 $x10^{11}$ $e^-$ $s^{-1}$ $cm^{-2}$ for 200 s to 2000 s, respectively. For the accumulated dose of $1x10^{16}$ $e^-$ $cm^{-2}$, the irradiation dose was 1 $x10^{12}$ $e^-$ $s^{-1}$ $cm^{-2}$ for 10000 s. The perovskite thin-films were irradiated through the encapsulating PMMA layer. After the irradiation experiments the solar cells were shipped back to Valencia and characterized again.

Acknowledgements:

The research leading to these results has received funding from the European Research Council (ERC) under the European Union's Horizon 2020 research and innovation programme (Grant agreement No. 834431 and No. 648433), the Spanish Ministry of Science, Innovation and Universities (MINECO), MAT2017-88821-R, PCI2019-111829-2 and EQC2018-004888-P and the Comunitat Valenciana IDIFEDER/2018/061 and Prometeu/2020/077. The project that gave rise to these results received the support of a fellowship from "la Caixa" Foundation (ID 100010434). The fellowship code is LCF/BQ/DI19/11730020.

References.

(1) Kojima, A.; Teshima, K.; Shirai, Y.; Miyasaka, T. Organometal Halide Perovskites as Visible-Light Sensitizers for Photovoltaic Cells. *J. Am. Chem. Soc.* **2009**, *131* (17), 6050–6051. https://doi.org/10.1021/ja809598r.

(2) Park, N.-G.; Zhu, K. Scalable Fabrication and Coating Methods for Perovskite Solar Cells and Solar Modules. *Nat. Rev. Mater.* **2020**. https://doi.org/10.1038/s41578-019-0176-2.

(3) Miyasaka, T. Lead Halide Perovskites in Thin Film Photovoltaics: Background and Perspectives. *Bull. Chem. Soc. Jpn.* **2018**, *91* (7), 1058–1068. https://doi.org/10.1246/bcsj.20180071.

(4) Forgács, D.; Gil-Escrig, L.; Perez-Del-Rey, D.; Momblona, C.; Werner, J.; Niesen, B.; Ballif, C.; Sessolo, M.; Bolink, H. J. Efficient Monolithic Perovskite/Perovskite Tandem Solar Cells. *Adv. Energy Mater.* **2017**, *7* (8). https://doi.org/10.1002/aenm.201602121.

(5) Tong, J.; Song, Z.; Kim, D. H.; Chen, X.; Chen, C.; Palmstrom, A. F.; Ndione, P. F.; Reese, M. O.; Dunfield, S. P.; Reid, O. G.; et al. Carrier Lifetimes of ≫1 Ms in Sn-Pb Perovskites Enable Efficient All-Perovskite Tandem Solar Cells. *Science (80-. ).* **2019**, *364*

(6439), 475 LP – 479. https://doi.org/10.1126/science.aav7911.

(6) Unger, E. L.; Kegelmann, L.; Suchan, K.; Sörell, D.; Korte, L.; Albrecht, S. Roadmap and Roadblocks for the Band Gap Tunability of Metal Halide Perovskites. *J. Mater. Chem. A* **2017**, *5* (23), 11401–11409. https://doi.org/10.1039/c7ta00404d.

(7) Wang, X.; Ling, Y.; Lian, X.; Xin, Y.; Dhungana, K. B.; Perez-Orive, F.; Knox, J.; Chen, Z.; Zhou, Y.; Beery, D.; et al. Suppressed Phase Separation of Mixed-Halide Perovskites Confined in Endotaxial Matrices. *Nat. Commun.* **2019**, *10* (1), 695. https://doi.org/10.1038/s41467-019-08610-6.

(8) Luo, D.; Su, R.; Zhang, W.; Gong, Q.; Zhu, R. Minimizing Non-Radiative Recombination Losses in Perovskite Solar Cells. *Nat. Rev. Mater.* **2020**, *5* (1), 44–60. https://doi.org/10.1038/s41578-019-0151-y.

(9) Yin, W.-J.; Shi, T.; Yan, Y. Unique Properties of Halide Perovskites as Possible Origins of the Superior Solar Cell Performance. *Adv. Mater.* **2014**, *26* (27), 4653–4658.

(10) Kaltenbrunner, M.; Adam, G.; Głowacki, E. D.; Drack, M.; Schwödiauer, R.; Leonat, L.; Apaydin, D. H.; Groiss, H.; Scharber, M. C.; White, M. S.; et al. Flexible High Power-per-Weight Perovskite Solar Cells with Chromium Oxide–Metal Contacts for Improved Stability in Air. *Nat. Mater.* **2015**, *14* (10), 1032–1039. https://doi.org/10.1038/nmat4388.

(11) Cardinaletti, I.; Vangerven, T.; Nagels, S.; Cornelissen, R.; Schreurs, D.; Hruby, J.; Vodnik, J.; Devisscher, D.; Kesters, J.; D'Haen, J.; et al. Organic and Perovskite Solar Cells for Space Applications. *Sol. Energy Mater. Sol. Cells* **2018**, *182*, 121–127. https://doi.org/10.1016/J.SOLMAT.2018.03.024.

(12) Klein-Kedem, N.; Cahen, D.; Hodes, G. Effects of Light and Electron Beam Irradiation on Halide Perovskites and Their Solar Cells. *Acc. Chem. Res.* **2016**, *49* (2), 347–354.

https://doi.org/10.1021/acs.accounts.5b00469.

(13) Huang, J.; Kelzenberg, M. D.; Espinet-González, P.; Mann, C.; Walker, D.; Naqavi, A.; Vaidya, N.; Warmann, E.; Atwater, H. A. Effects of Electron and Proton Radiation on Perovskite Solar Cells for Space Solar Power Application. In *2017 IEEE 44th Photovoltaic Specialist Conference (PVSC)*; 2017; pp 1248–1252. https://doi.org/10.1109/PVSC.2017.8366410.

(14) Miyazawa, Y.; Ikegami, M.; Chen, H.-W.; Ohshima, T.; Imaizumi, M.; Hirose, K.; Miyasaka, T. Tolerance of Perovskite Solar Cell to High-Energy Particle Irradiations in Space Environment. *iScience* **2018**, *2*, 148–155. https://doi.org/https://doi.org/10.1016/j.isci.2018.03.020.

(15) Paternò, G. M.; Robbiano, V.; Santarelli, L.; Zampetti, A.; Cazzaniga, C.; Garcìa Sakai, V.; Cacialli, F. Perovskite Solar Cell Resilience to Fast Neutrons. *Sustain. Energy Fuels* **2019**, *3* (10), 2561–2566. https://doi.org/10.1039/C9SE00102F.

(16) Yang, S.; Xu, Z.; Xue, S.; Kandlakunta, P.; Cao, L.; Huang, J. Organohalide Lead Perovskites: More Stable than Glass under Gamma-Ray Radiation. *Adv. Mater.* **2019**, *31* (4), 1805547. https://doi.org/10.1002/adma.201805547.

(17) Hentz, O.; Zhao, Z.; Gradečak, S. Impacts of Ion Segregation on Local Optical Properties in Mixed Halide Perovskite Films. *Nano Lett.* **2016**, *16* (2), 1485–1490. https://doi.org/10.1021/acs.nanolett.5b05181.

(18) Xiao, C.; Li, Z.; Guthrey, H.; Moseley, J.; Yang, Y.; Wozny, S.; Moutinho, H.; To, B.; Berry, J. J.; Gorman, B.; et al. Mechanisms of Electron-Beam-Induced Damage in Perovskite Thin Films Revealed by Cathodoluminescence Spectroscopy. *J. Phys. Chem. C* **2015**, *119* (48), 26904–26911. https://doi.org/10.1021/acs.jpcc.5b09698.

(19) Song, Z.; Li, C.; Chen, C.; McNatt, J.; Yoon, W.; Scheiman, D.; Jenkins, P. P.; Ellingson, R.

J.; Heben, M. J.; Yan, Y. High Remaining Factors in the Photovoltaic Performance of Perovskite Solar Cells after High-Fluence Electron Beam Irradiations. *J. Phys. Chem. C* **2020**, *124* (2), 1330–1336. https://doi.org/10.1021/acs.jpcc.9b11483.

(20) Malinkiewicz, O.; Yella, A.; Lee, Y. H.; Espallargas, G. M. M.; Graetzel, M.; Nazeeruddin, M. K.; Bolink, H. J. Perovskite Solar Cells Employing Organic Charge-Transport Layers. *Nat. Photonics* **2014**, *8* (February), 128–132. https://doi.org/10.1038/nphoton.2013.341.

(21) Pérez-del-Rey, D.; Gil-Escrig, L.; Zanoni, K. P. S.; Dreessen, C.; Sessolo, M.; Boix, P. P.; Bolink, H. J. Molecular Passivation of MoO3: Band Alignment and Protection of Charge Transport Layers in Vacuum-Deposited Perovskite Solar Cells. *Chem. Mater.* **2019**, *31* (17), 6945–6949. https://doi.org/10.1021/acs.chemmater.9b01396.

(22) Schulman, J. H.; Compton, W. D. *Color Centers in Solids*; Pergamon Press Macmillan: New York, 1962.

(23) Hamache, A.; Sengouga, N.; Meftah, A.; Henini, M. Modeling the Effect of 1MeV Electron Irradiation on the Performance of N+–p–P+ Silicon Space Solar Cells. *Radiat. Phys. Chem.* **2016**, *123*, 103–108. https://doi.org/https://doi.org/10.1016/j.radphyschem.2016.02.025.

(24) Danilchenko, B.; Budnyk, A.; Shpinar, L.; Poplavskyy, D.; Zelensky, S. E.; Barnham, K. W. J.; Ekins-Daukes, N. J. 1MeV Electron Irradiation Influence on GaAs Solar Cell Performance. *Sol. Energy Mater. Sol. Cells* **2008**, *92* (11), 1336–1340. https://doi.org/https://doi.org/10.1016/j.solmat.2008.05.006.

(25) Parravicini, J.; Arcadi, F.; Le Donne, A.; Campesato, R.; Casale, M.; Greco, E.; Binetti, S. Effect of the Irradiation on Optical and Electrical Properties of Triple-Junction Flexible Thin Solar Cells for Space Applications . *Frontiers in Physics* . 2019, p 169.

(26) Bätzner, D. L.; Romeo, A.; Terheggen, M.; Döbeli, M.; Zogg, H.; Tiwari, A. N. Stability Aspects in CdTe/CdS Solar Cells. *Thin Solid Films* **2004**, *451–452*, 536–543. https://doi.org/https://doi.org/10.1016/j.tsf.2003.10.141.

(27) Rau, Uwe, Jaseneck, A, Schock, H. W. et. al. Radiation Induced Defects In Cu(Ln,Ga)Se Solar Cells – Comparison of Electrical and Proton Irradiation. *28th IEEE PVSC Anchorage* **2000**, 1032.

(28) Momblona, C.; Gil-Escrig, L.; Bandiello, E.; Hutter, E. M.; Sessolo, M.; Lederer, K.; Blochwitz-Nimoth, J.; Bolink, H. J. Efficient Vacuum Deposited P-i-n and n-i-p Perovskite Solar Cells Employing Doped Charge Transport Layers. *Energy Environ. Sci.* **2016**, *9* (11), 3456–3463. https://doi.org/10.1039/C6EE02100J.